Emergence of Spinons in Layered Trimer Iridate $Ba_4Ir_3O_{10}$

Y. Shen,[1,*] J. Sears,[1] G. Fabbris,[2] A. Weichselbaum,[1] W. Yin,[1] H. Zhao,[3] D. G. Mazzone,[4] H. Miao,[1,5] M. H. Upton,[2] D. Casa,[2] R. Acevedo-Esteves,[6] C. Nelson,[6] A. M. Barbour,[6] C. Mazzoli,[6] G. Cao,[3] and M. P. M. Dean[1,†]

[1]*Condensed Matter Physics and Materials Science Department, Brookhaven National Laboratory, Upton, New York 11973, USA*
[2]*Advanced Photon Source, Argonne National Laboratory, Argonne, Illinois 60439, USA*
[3]*Department of Physics, University of Colorado Boulder, Boulder, Colorado 80309, USA*
[4]*Laboratory for Neutron Scattering and Imaging, Paul Scherrer Institut, CH-5232 Villigen, Switzerland*
[5]*Material Science and Technology Division, Oak Ridge National Laboratory, Oak Ridge, Tennessee 37830, USA*
[6]*National Synchrotron Light Source II, Brookhaven National Laboratory, Upton, New York 11973, USA*

(Received 4 January 2022; accepted 17 October 2022; published 10 November 2022)

Spinons are well known as the elementary excitations of one-dimensional antiferromagnetic chains, but means to realize spinons in higher dimensions is the subject of intense research. Here, we use resonant x-ray scattering to study the layered trimer iridate $Ba_4Ir_3O_{10}$, which shows no magnetic order down to 0.2 K. An emergent one-dimensional spinon continuum is observed that can be well described by XXZ spin-1/2 chains with a magnetic exchange of ∼55 meV and a small Ising-like anisotropy. With 2% isovalent Sr doping, magnetic order appears below $T_N = 130$ K along with sharper excitations in $(Ba_{1-x}Sr_x)_4Ir_3O_{10}$. Combining our data with exact diagonalization calculations, we find that the frustrated intratrimer interactions effectively reduce the system into decoupled spin chains, the subtle balance of which can be easily tipped by perturbations such as chemical doping. Our results put $Ba_4Ir_3O_{10}$ between the one-dimensional chain and two-dimensional quantum spin liquid scenarios, illustrating a new way to suppress magnetic order and realize fractional spinons.

DOI: 10.1103/PhysRevLett.129.207201

Quantum spin liquids (QSLs) are novel states of matter where quantum fluctuations prevent symmetry breaking down to zero temperature [1–6]. A key characteristic of QSLs is that they can host fractional elementary excitations called spinons, carrying spin-1/2, which can serve as a fingerprint for these states. Arguably the best-understood example of this is a one-dimensional (1D) spin-1/2 antiferromagnetic (AFM) chain where the spinons describe the spin domain wall dynamics [7–15]. QSLs in higher dimensions are harder to identify, but hold promise for realizing novel topological order and intrinsic long-range quantum entanglement with potential applications in quantum information [16,17]. Several studies have provided evidence for spinons in two-dimensional (2D) or three-dimensional (3D) systems such as triangular, kagome, Kitaev honeycomb, or pyrochlore lattices [18–23], while definitive material realization remains controversial and is a major target of research. Another possible approach relies on 1D systems as building blocks to realize higher-dimensional QSL states [24], which, however, is less explored.

The insulating magnet $Ba_4Ir_3O_{10}$ is an intriguing candidate for realizing novel mechanisms for the emergence of spinons [25–28]. As shown in Fig. 1(a), it has a quasi-2D structure composed of buckled sheets with a Ir $5d^5$ nominal atomic configuration. Each sheet constitutes corner-connected Ir_3O_{12} trimers containing three distorted face-sharing IrO_6 octahedra. The shortest Ir-Ir bond is the one between Ir1 and Ir2 within a trimer, which has a length of ∼2.58 Å [25,29], shorter than that of elemental iridium (∼2.71 Å [30]). Thus, strong intratrimer couplings are expected, such as those found in other face-sharing iridates [31–34], and isostructural $Ba_4Ru_3O_{10}$ [35–40]. This directly leads to a strong nearest neighbor (NN) exchange interaction J_1 within each trimer [see Fig. 1(a)]. Another intratrimer interaction is the third NN term J_3, which can be realized by the superexchange path through the Ir2 ion. The Ir1 ions are also connected through the second NN interaction J_2, forming zigzag chains along the crystalline c direction. All other magnetic interactions can be ignored due to the long bond lengths and unfavorable hopping trajectories. Considering the expectation of appreciable magnetic exchange and the lack of any obvious magnetic frustration, this material would be expected to be a long-range ordered antiferromagnet. Previous transport and magnetization studies found no magnetic order down to 0.2 K despite a Curie-Weiss temperature up to −766 K [25]. In contrast, the material shows a linear behavior in the low-temperature magnetic heat capacity [25], resembling a gapless QSL [41,42]. In fact, the ground state is rather susceptible to perturbations including sample growth conditions and chemical doping [25–27]. The origin of the highly suppressed magnetic order and fragile ground state remains puzzling and cannot be solved without direct measurements of the magnetic excitation spectrum.

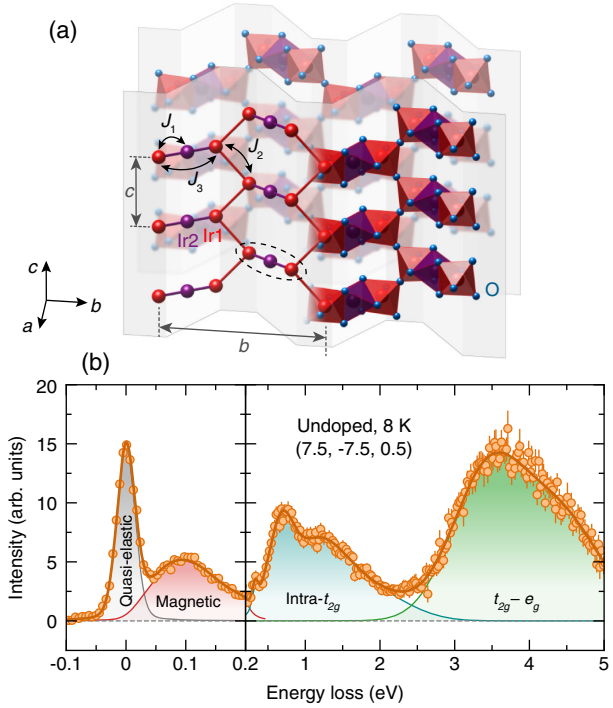

FIG. 1. (a) Crystal structure of $Ba_4Ir_3O_{10}$. The material contains two symmetry-inequivalent Ir ions: Ir1 and Ir2, occupying the outer and middle sites of the trimers (black dashed ellipse), respectively. J_n where $n = 1, 2, 3$ denotes magnetic interactions for the first, second, and third nearest Ir neighbors. The barium ions are not shown. (b) Representative RIXS spectrum of $Ba_4Ir_3O_{10}$ at the Ir L_3 edge with a constant background subtracted. The circles represent the data and the different lines with shaded areas indicate the fitting results of different components, the summation of which gives the dark orange curve. Error bars represent 1 standard deviation based on Poisson statistics.

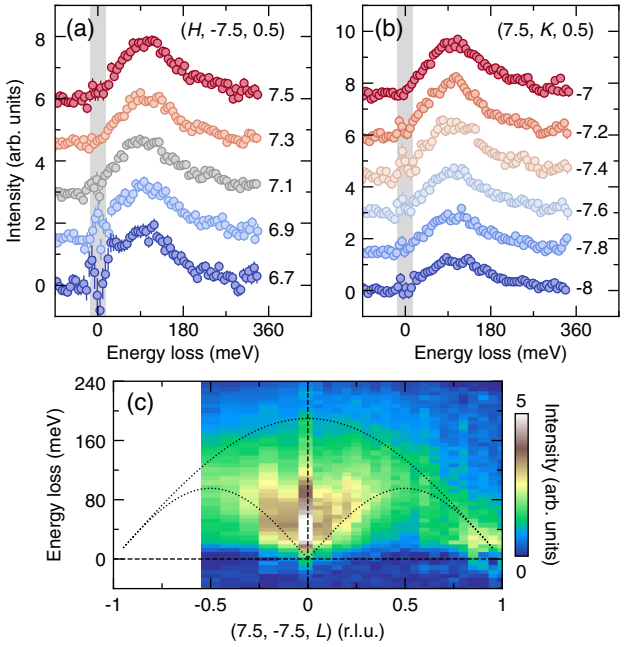

FIG. 2. One-dimensional spinons in undoped $Ba_4Ir_3O_{10}$ at 8 K. (a),(b) Magnetic excitations at different $\boldsymbol{Q}$ along H and K directions, respectively, showing essentially dispersionless behavior. All the RIXS spectra in the text are presented with the constant background, quasielastic line and high-energy dd excitations subtracted to highlight the magnetic contributions [43]. The vertical gray bars indicate the quasielastic regime, the widths of which represent the energy resolution. The values of H/K are indicated for each curve and the spectra are shifted along the y axis for clarity. (c) Color plot of the magnetic excitations along the L direction. The dotted lines are the calculated excitation boundaries of an AFM spin-1/2 chain with $J_{\text{chain}} = 55$ meV and $\Delta = 1.3$. The dashed lines are guides to the eye.

In this Letter, we use resonant inelastic x-ray scattering (RIXS) at the Ir L_3 edge and resonant elastic x-ray scattering (REXS) at the O K edge to study the magnetic properties of $Ba_4Ir_3O_{10}$. For comparison, we also measure the isovalently doped $(Ba_{1-x}Sr_x)_4Ir_3O_{10}$ $(x = 0.02)$, in which a small amount of Sr doping surprisingly triggers magnetic order below 130 K. 1D continuous spinon excitations are discovered in undoped $Ba_4Ir_3O_{10}$ which can be well described by a spin-1/2 XXZ AFM chain with small Ising-like anisotropy. In contrast, $(Ba_{1-x}Sr_x)_4Ir_3O_{10}$ shows magnetic order with a propagation vector of (0.5, 0, 0), and a comparably sharp dispersion, which remains 1D-like down to base temperature. Through exact diagonalization (ED) calculations, we show that the zigzag chains retained by J_2 are effectively decoupled at a critical point triggered by the competition between the interchain interactions J_1 and J_3, the balance of which can be easily tipped by perturbations.

RIXS data were collected at the Ir L_3 edge with a horizontal scattering plane and π polarization and energy resolution of about 32 meV [43]. Wave vectors throughout the manuscript are defined using standard reciprocal lattice units (r.l.u.) notation as $\boldsymbol{Q} = H\mathbf{a}^* + K\mathbf{b}^* + L\mathbf{c}^*$ based on lattice constants $a = 7.2545$ Å, $b = 13.192$ Å, $c = 5.7737$ Å, $\alpha = \gamma = 90°$, $\beta = 113.513°$.

Figure 1(b) displays a representative Ir L_3 edge RIXS spectrum at 11.215 keV composed of a quasielastic peak, low-energy magnetic excitations, and high-energy dd excitations of both intra-t_{2g} orbitals and from t_{2g} to e_g orbitals. The overall form of the spectrum is consistent with expectations for Ir $5d^5$ materials [50,51]. We further checked for possible intratrimer charge disproportionation via bond valence sum analysis and found it to be negligible [43]. To separate the spectral components we fit the spectra with different functions. The quasielastic peak can be represented by a pseudo-Voigt profile with a width dominated by the energy resolution. The low symmetry of $Ba_4Ir_3O_{10}$ implies that the magnetic and crystal field excitations are unlikely to have theoretically rigorous analytical forms. We find that phenomenological forms of a damped harmonic oscillator convoluted with the resolution and a manifold of pseudo-Voigts can represent

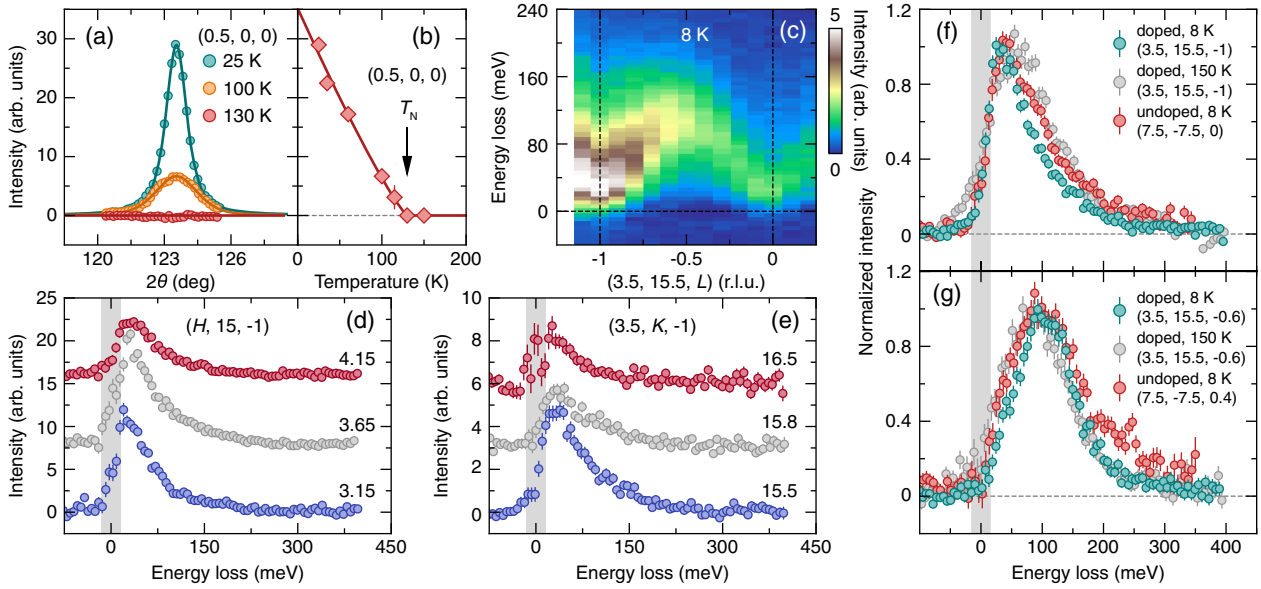

FIG. 3. Magnetic order and spin dynamics in doped $(Ba_{1-x}Sr_x)_4Ir_3O_{10}$ $(x = 0.02)$ and comparison with undoped $Ba_4Ir_3O_{10}$. (a) Background subtracted magnetic Bragg peaks at $\boldsymbol{Q} = (0.5, 0, 0)$, detected at the O K edge with different temperatures in $(Ba_{1-x}Sr_x)_4Ir_3O_{10}$. The solid lines are the fitting results using pseudo-Voigt profiles [43]. (b) Temperature dependence of the fitted peak height. The magnetic transition takes place at $T_N = 130$ K. The solid and dashed lines are guides to the eye. (c)–(e) Magnetic excitation spectra of $(Ba_{1-x}Sr_x)_4Ir_3O_{10}$ at 8 K with different $\boldsymbol{Q}$ along L, H, and K directions, respectively. (f),(g) Magnetic excitation spectra at different temperatures for $Ba_4Ir_3O_{10}$ and $(Ba_{1-x}Sr_x)_4Ir_3O_{10}$ samples. The intensities are normalized according to their maximum values. Note that $(3.5, 15.5, -1)$ and $(7.5, -7.5, 0)$ are symmetric regarding the chain direction. The observed phase shift in the spinon spectrum with respect to L arises from zone folding caused by the interchain interactions and the sampling of different chains with changes in $\boldsymbol{Q}$ [9]. The same applies to $(3.5, 15.5, -0.6)$ and $(7.5, -7.5, 0.4)$. The dashed lines are guides to the eye and the quasielastic regime is indicated by the vertical gray bars.

the magnetic and dd excitations, respectively, as shown by the fit lines in Fig. 1(b) [43]. These phenomenological forms for the quasielastic line and intra-t_{2g} excitations will be used later to isolate the magnetic scattering which is the main focus of this Letter.

We start with the magnetic excitations in undoped $Ba_4Ir_3O_{10}$ along different momentum directions. Our sample comes from the same batch studied in Ref. [25] that show no magnetic transition down to 0.2 K. As plotted in Figs. 2(a) and 2(b), both the energies and line shapes are essentially dispersionless in $(H, 0, 0)$ and $(0, K, 0)$ directions. In contrast, dispersive excitations are revealed along the L direction [Fig. 2(c)]. Intriguingly, the excitations are very broad along the energy loss axis, distinct from sharp spin waves, rather resembling the magnetic continuum consistent with spinons. A gaplike feature is observed with intensity maximum around 40 meV, consistent with the anisotropy revealed by magnetization [25]. Considering the 1D character of the dispersion, we propose a spin-1/2 XXZ AFM chain Hamiltonian

$$\mathcal{H} = J_{\text{chain}} \sum_{\langle ij \rangle} [S_i^x S_j^x + S_i^y S_j^y + \Delta S_i^z S_j^z], \qquad (1)$$

where J_{chain} is the NN intrachain interactions, which corresponds to J_2 in our case connecting the Ir1 atoms, $\langle ij \rangle$ denotes bond sums along the chain, and Δ controls the interaction anisotropy. We calculated the zero temperature two-spinon response with $J_{\text{chain}} = 55$ meV and $\Delta = 1.3$ and plot the result in Fig. 2(c) and Supplemental Material Fig. S5 [43,52]. This provides a satisfactory description of all the major features of the data, indicating that, despite the 2D structure of $Ba_4Ir_3O_{10}$, its magnetic dynamics can be well described by the continuous spinon excitations of 1D AFM chains.

To test the fragility of the QSL state, we turn to the isovalently doped $(Ba_{1-x}Sr_x)_4Ir_3O_{10}$ $(x = 0.02)$ which has been previously reported to show a magnetic transition below $T_N = 130$ K [25]. We used O K edge REXS measurements to test for the presence of order and reveal a magnetic Bragg peak at $\boldsymbol{Q} = (0.5, 0, 0)$ [Figs. 3(a) and 3(b)], which disappears above $T_N = 130$ K, consistent with the thermodynamic results [25]. Regarding the magnetic excitations, similar to the undoped $Ba_4Ir_3O_{10}$, no dispersion can be distinguished along the H and K directions in $(Ba_{1-x}Sr_x)_4Ir_3O_{10}$, while clear $\boldsymbol{Q}$ dependence is discovered along the L direction at 8 K [Figs. 3(c)–3(e)]. A gaplike feature is also observed, consistent with its slight Ising-type anisotropy. However, further analysis of the gap structure, and its correspondence to the heat capacity data, is impeded by the limited energy resolution here. Above T_N, the excitations become broader and less dispersive

[Figs. 3(f) and 3(g)]. The flattening of the dispersion is in line with the Ising spin nature.

It has been theoretically proposed that the oxygen-mediated electronic hopping between face-sharing Ir octahedra can be extremely weak under certain circumstances [53], leading to vanishing J_1 superexchange parameters, naturally decoupling the zigzag chains running along the c direction in $Ba_4Ir_3O_{10}$. However, this weak coupling model does not take into account the direct hoppings between the neighboring Ir ions which tend to be significant for face-sharing octahedra [31–40]. Indeed, the Bonner-Fisher peak in the susceptibility expected for 1D systems [54,55], is absent in $Ba_4Ir_3O_{10}$ [25]. Furthermore, compared with undoped $Ba_4Ir_3O_{10}$, the excitations in magnetically ordered $(Ba_{1-x}Sr_x)_4Ir_3O_{10}$ have similarly shaped dispersion but are somewhat sharper in energy [Figs. 3(f) and 3(g)]. This behavior differs from that expected for the weak coupling model, where the weak interchain coupling leads to multiple bound triplon states in addition to the spinon continuum [9,24,56,57]. Such inconsistency leads us to another explanation, a strong coupling model [58,59], where the intratrimer AFM interactions J_1 and J_3 are substantial and compete with each other, effectively decoupling the chains.

To understand the origin of the frustration between J_1 and J_3, we make use of cluster ED calculations utilizing the EDRIXS software [60,61]. We represent the trimer units in $Ba_4Ir_3O_{10}$ using a cluster model with three Ir sites with Coulomb interactions and interatomic d-d hopping explicitly taken into account through Slater-Koster parametrization [43]. For each Ir site with a nominal $5d^5$ configuration, the ground state is an $S_{\mathrm{eff}} = 1/2$ doublet. These $S_{\mathrm{eff}} = 1/2$ states recombine in the cluster to yield four Kramers doublets: an antisymmetric doublet $|S = 1/2\rangle^-$, a symmetric doublet $|S = 1/2\rangle^+$, and a high-spin multiplet $|S = 3/2\rangle$ which can further split into $|S = 3/2, S_z = \pm 1/2\rangle$ and $|S = 3/2, S_z = \pm 3/2\rangle$ in the presence of anisotropic interactions [43]. As shown in Fig. 4(a), with increasing inter-Ir-site hopping, the energies of $|S = 3/2, S_z = \pm 1/2\rangle$ and $|S = 3/2, S_z = \pm 3/2\rangle$ increase monotonically. The fact that the $|S = 3/2, S_z = \pm 3/2\rangle$ doublet lies at higher energy indicates Ising-like anisotropy for the intratrimer interactions. In contrast, $|S = 1/2\rangle^-$ and $|S = 1/2\rangle^+$ show strong competition and the ground state switches between these two doublets at a critical point of $V_{dd\sigma} \approx 0.8$ eV.

The presence of the critical point directly leads to the effective decoupling of the spin chains. Assuming an $|S = 1/2\rangle^-$ ground state for all the trimers (the real ground state is a superposition of $|S = 1/2\rangle^+$ and $|S = 1/2\rangle^-$ at the critical point), the RIXS process leads to a single spin flip at one of the Ir sites [Fig. 4(b)], which at low energies turns the corresponding trimer from $|S = 1/2\rangle^-$ to $|S = 1/2\rangle^+$, leaving two spinons (domain walls) in the zigzag spin chain. As the spinons propagate along the chain, the neighboring spins are flipped, switching the trimers between $|S = 1/2\rangle^-$ and $|S = 1/2\rangle^+$ [Fig. 4(c)]. At the

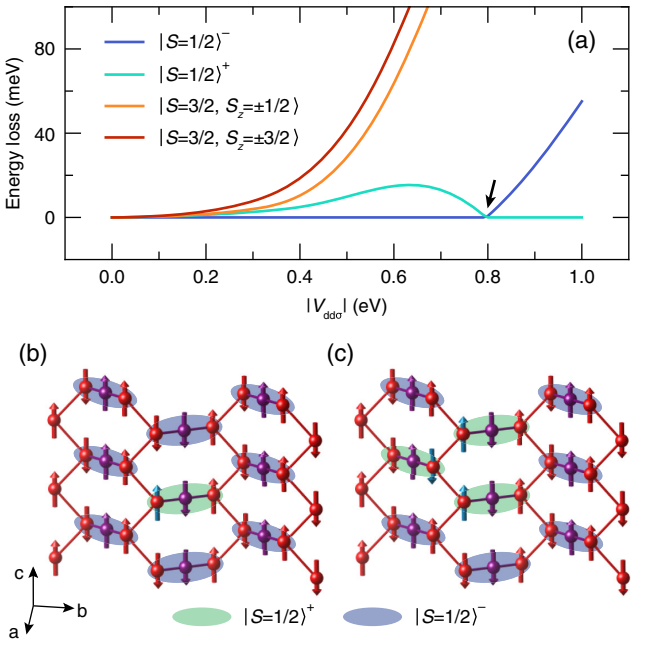

FIG. 4. Effective chain decoupling. (a) Low-energy spectrum of the three-Ir-site cluster model as a function of intersite d-d hopping [43]. The black arrow highlights the critical point where the $|S = 1/2\rangle^+$ and $|S = 1/2\rangle^-$ doublets are degenerate. (b) During the RIXS process, one Ir spin is flipped (cyan arrow), changing the trimer state at low energies and creating two spinons (domain walls). (c) The spinons can propagate in the zigzag chain along the c direction by flipping the neighboring spins.

critical point, as the $|S = 1/2\rangle^-$ and $|S = 1/2\rangle^+$ doublets are degenerate, such events have no energy cost so that the spinons are deconfined and can propagate freely. Thus, the properties of undoped $Ba_4Ir_3O_{10}$ are naturally explained if it sits right at the critical point, resulting in emergent 1D behavior and continuous excitations observed in RIXS spectra. The delicate balance between competing interactions can be disrupted easily. In $(Ba_{1-x}Sr_x)_4Ir_3O_{10}$), the isovalent Sr doping leads to small structural changes and drives the system slightly away from the critical point so that the spinons become confined since the energy cost to switch between $|S = 1/2\rangle^-$ and $|S = 1/2\rangle^+$ doublets is no longer zero. Such behavior differs from the conventional doping effect where the dopants could enhance disorder and randomness, which tends to suppress magnetic order and promote glassy physics [62]. It should be noted that the Ising-like anisotropy in $(Ba_{1-x}Sr_x)_4Ir_3O_{10}$ makes it free from the constraints of the Mermin-Wagner theorem which requires a continuous symmetry. Thus, magnetic order does not necessarily imply finite interlayer coupling, although our diffraction measurements show H-axis correlations proving that interlayer coupling is present. A recent REXS experiment reports a 25 K magnetic transition in the undoped $Ba_4Ir_3O_{10}$ with a similar propagation vector as we found in the doped $(Ba_{1-x}Sr_x)_4Ir_3O_{10}$ [27].

The origin of this discrepancy is unclear, but it could indicate enhanced disorder.

The strong coupling model puts $Ba_4Ir_3O_{10}$ in between the 1D spin chains and 2D QSLs. Although its magnetic dynamics behave as 1D spinon excitations, the underlying magnetism is mostly 2D. Consequently, some of the characteristic features for a 1D system are missing such as the Bonner-Fisher peak in susceptibility and bound state upon ordering. The 1D behavior is caused by the emergent dimensional reduction due to magnetic frustration, which has also been reported in other materials [63]. This raises an interesting question of whether the properties relevant to 2D QSLs are preserved in this case, which is yet to be explored. Measurements of quantum entanglement, such as entanglement witnesses, could prove useful in this regard [22].

In summary, we use RIXS to show that emergent 1D spinon excitations can arise from the 2D magnetism in $Ba_4Ir_3O_{10}$ due to the frustrated interchain (intratrimer) interactions. The highly suppressed magnetic order can be easily recovered by disturbing the subtle balance of the frustration, confining the spinons into magnons. Although prior work has speculated that $Ba_4Ir_3O_{10}$ could be either a Luttinger liquid QSL or a 2D QSL such as a spinon Fermi surface states [25], the data here are the first evidence of a 1D spinon continuum in $Ba_4Ir_3O_{10}$. These results indicate that, instead of forming an isotropic QSL state, magnetic frustration can effectively reduce the system dimension, suppressing the magnetic order and realizing deconfined spinons in a unique way.

The supporting data for the plots in this article are openly available from the Zenodo database [64].

We thank Emil Bozin and Kemp Plumb for insightful conversations. Work at Brookhaven National Laboratory was supported by the U.S. Department of Energy, Office of Science, Office of Basic Energy Sciences. G. C. acknowledges NSF support via Grants No. DMR 1903888 and DMR 2204811. This research used resources of the Advanced Photon Source, a U.S. Department of Energy (DOE) Office of Science User Facility at Argonne National Laboratory and is based on research supported by the U.S. DOE Office of Science-Basic Energy Sciences, under Contract No. DE-AC02-06CH11357. This research used resources at the Coherent Soft X-Ray and *In Situ* and Resonant Hard X-Ray Studies beamline of the National Synchrotron Light Source II, a U.S. Department of Energy (DOE) Office of Science User Facility operated for the DOE Office of Science by Brookhaven National Laboratory under Contract No. DE-SC0012704.

*yshen@bnl.gov
†mdean@bnl.gov

[1] P. W. Anderson, Resonating valence bonds: A new kind of insulator?, Mater. Res. Bull. **8**, 153 (1973).
[2] P. W. Anderson, The resonating valence bond state in La_2CuO_4 and superconductivity, Science **235**, 1196 (1987).
[3] L. Balents, Spin liquids in frustrated magnets, Nature (London) **464**, 199 (2010).
[4] L. Savary and L. Balents, Quantum spin liquids: A review, Rep. Prog. Phys. **80**, 016502 (2017).
[5] Y. Zhou, K. Kanoda, and T.-K. Ng, Quantum spin liquid states, Rev. Mod. Phys. **89**, 025003 (2017).
[6] C. Broholm, R. Cava, S. Kivelson, D. Nocera, M. Norman, and T. Senthil, Quantum spin liquids, Science **367**, 263 (2020).
[7] B. Lake, D. A. Tennant, C. D. Frost, and S. E. Nagler, Quantum criticality and universal scaling of a quantum antiferromagnet, Nat. Mater. **4**, 329 (2005).
[8] M. Mourigal, M. Enderle, A. Klopperpieper, J.-S. Caux, A. Stunault, and H. M. Rønnow, Fractional spinon excitations in the quantum Heisenberg antiferromagnetic chain, Nat. Phys. **9**, 435 (2013).
[9] A. K. Bera, B. Lake, F. H. L. Essler, L. Vanderstraeten, C. Hubig, U. Schollwöck, A. T. M. N. Islam, A. Schneidewind, and D. L. Quintero-Castro, Spinon confinement in a quasi-one-dimensional anisotropic Heisenberg magnet, Phys. Rev. B **96**, 054423 (2017).
[10] Q. Faure, S. Takayoshi, S. Petit, V. Simonet, S. Raymond, L.-P. Regnault, M. Boehm, J. S. White, M. Månsson, C. Rüegg, P. Lejay, B. Canals, T. Lorenz, S. C. Furuya, T. Giamarchi, and B. Grenier, Topological quantum phase transition in the Ising-like antiferromagnetic spin chain $BaCo_2V_2O_8$, Nat. Phys. **14**, 716 (2018).
[11] Q. Faure, S. Takayoshi, V. Simonet, B. Grenier, M. Månsson, J. S. White, G. S. Tucker, C. Rüegg, P. Lejay, T. Giamarchi, and S. Petit, Tomonaga-Luttinger Liquid Spin Dynamics in the Quasi-One-Dimensional Ising-Like Antiferromagnet $BaCo_2V_2O_8$, Phys. Rev. Lett. **123**, 027204 (2019).
[12] J. Schlappa, K. Wohlfeld, K. J. Zhou, M. Mourigal, M. W. Haverkort, V. N. Strocov, L. Hozoi, C. Monney, S. Nishimoto, S. Singh, A. Revcolevschi, J. S. Caux, L. Patthey, H. M. Rønnow, J. van den Brink, and T. Schmitt, Spin-orbital separation in the quasi-one-dimensional Mott insulator Sr_2CuO_3, Nature (London) **485**, 82 (2012).
[13] V. Bisogni, K. Wohlfeld, S. Nishimoto, C. Monney, J. Trinckauf, K. Zhou, R. Kraus, K. Koepernik, C. Sekar, V. Strocov, B. Büchner, T. Schmitt, J. van den Brink, and J. Geck, Orbital Control of Effective Dimensionality: From Spin-Orbital Fractionalization to Confinement in the Anisotropic Ladder System $CaCu_2O_3$, Phys. Rev. Lett. **114**, 096402 (2015).
[14] U. Kumar, A. Nag, J. Li, H. C. Robarts, A. C. Walters, M. García-Fernández, R. Saint-Martin, A. Revcolevschi, J. Schlappa, T. Schmitt, S. Johnston, and K.-J. Zhou, Unraveling higher-order contributions to spin excitations probed using resonant inelastic x-ray scattering, Phys. Rev. B **106**, L060406 (2022).
[15] M. Rossi, P. Marabotti, Y. Hirata, G. Monaco, M. Krisch, K. Ohgushi, K. Wohlfeld, J. van den Brink, and M. Moretti Sala, A $j_{\mathrm{eff}} = 1/2$ pseudospinon continuum in $CaIrO_3$, Eur. Phys. J. Plus **135**, 676 (2020).
[16] X.-G. Wen, Quantum orders and symmetric spin liquids, Phys. Rev. B **65**, 165113 (2002).

[17] L. B. Ioffe, M. V. Feigel'man, A. Ioselevich, D. Ivanov, M. Troyer, and G. Blatter, Topologically protected quantum bits using Josephson junction arrays, Nature (London) **415**, 503 (2002).

[18] T.-H. Han, J. S. Helton, S. Chu, D. G. Nocera, J. A. Rodriguez-Rivera, C. Broholm, and Y. S. Lee, Fractionalized excitations in the spin-liquid state of a kagome-lattice antiferromagnet, Nature (London) **492**, 406 (2012).

[19] Y. Shen, Y.-D. Li, H. Wo, Y. Li, S. Shen, B. Pan, Q. Wang, H. C. Walker, P. Steffens, M. Boehm, Y. Hao, D. L. Quintero-Castro, L. W. Harriger, M. D. Frontzek, L. Hao, S. Meng, Q. Zhang, G. Chen, and J. Zhao, Evidence for a spinon Fermi surface in a triangular-lattice quantum-spin-liquid candidate, Nature (London) **540**, 559 (2016).

[20] B. Gao *et al.*, Experimental signatures of a three-dimensional quantum spin liquid in effective spin-1/2 $Ce_2Zr_2O_7$ pyrochlore, Nat. Phys. **15**, 1052 (2019).

[21] L. Martinelli, D. Betto, K. Kummer, R. Arpaia, L. Braicovich, D. Di Castro, N. B. Brookes, M. Moretti Sala, and G. Ghiringhelli, Fractional Spin Excitations in the Infinite-Layer Cuprate $CaCuO_2$, Phys. Rev. X **12**, 021041 (2022).

[22] A. O. Scheie, E. A. Ghioldi, J. Xing, J. A. M. Paddison, N. E. Sherman, M. Dupont, D. Abernathy, D. M. Pajerowski, S.-S. Zhang, L. O. Manuel, A. E. Trumper, C. D. Pemmaraju, A. S. Sefat, D. S. Parker, T. P. Devereaux, J. E. Moore, C. D. Batista, and D. A. Tennant, Witnessing quantum criticality and entanglement in the triangular antiferromagnet $KYbSe_2$, arXiv:2109.11527.

[23] A. Banerjee, J. Yan, J. Knolle, C. A. Bridges, M. B. Stone, M. D. Lumsden, D. G. Mandrus, D. A. Tennant, R. Moessner, and S. E. Nagler, Neutron scattering in the proximate quantum spin liquid α-$RuCl_3$, Science **356**, 1055 (2017).

[24] M. Kohno, O. A. Starykh, and L. Balents, Spinons and triplons in spatially anisotropic frustrated antiferromagnets, Nat. Phys. **3**, 790 (2007).

[25] G. Cao, H. Zheng, H. Zhao, Y. Ni, C. A. Pocs, Y. Zhang, F. Ye, C. Hoffmann, X. Wang, M. Lee, M. Hermele, and I. Kimchi, Quantum liquid from strange frustration in the trimer magnet $Ba_4Ir_3O_{10}$, npj Quantum Mater. **5**, 26 (2020).

[26] G. Cao, H. Zhao, B. Hu, N. Pellatz, D. Reznik, P. Schlottmann, and I. Kimchi, Quest for quantum states via field-altering technology, npj Quantum Mater. **5**, 83 (2020).

[27] X. Chen, Y. He, S. Wu, Y. Song, D. Yuan, E. Bourret-Courchesne, J. P. C. Ruff, Z. Islam, A. Frano, and R. J. Birgeneau, Structural and magnetic transitions in the planar antiferromagnet $Ba_4Ir_3O_{10}$, Phys. Rev. B **103**, 224420 (2021).

[28] A. Sokolik, S. Hakani, S. Roy, N. Pellatz, H. Zhao, G. Cao, I. Kimchi, and D. Reznik, Spinons and damped phonons in spin-1/2 quantum-liquid $Ba_4Ir_3O_{10}$ observed by Raman scattering, Phys. Rev. B **106**, 075108 (2022).

[29] K. E. Stitzer, M. D. Smith, and H.-C. zur Loye, Crystal growth, structure determination and magnetic properties of $Ba_4Ir_3O_{10}$ and $Ba_4(Co_{0.4}Ir_{0.6})Ir_2O_{10}$, J. Alloys Compd. **338**, 104 (2002).

[30] R. Wyckoff, *Crystal Structures* (Wiley, New York, 1963).

[31] I. Terasaki, S. Ito, T. Igarashi, S. Asai, H. Taniguchi, R. Okazaki, Y. Yasui, K. Kobayashi, R. Kumai, H. Nakao, and Y. Murakami, Novel charge ordering in the trimer iridium oxide $BaIrO_3$, Crystals **6**, 27 (2016).

[32] R. Okazaki, S. Ito, K. Tanabe, H. Taniguchi, Y. Ikemoto, T. Moriwaki, and I. Terasaki, Spectroscopic signature of trimer Mott insulator and charge disproportionation in $BaIrO_3$, Phys. Rev. B **98**, 205131 (2018).

[33] M. Ye, H.-S. Kim, J.-W. Kim, C.-J. Won, K. Haule, D. Vanderbilt, S.-W. Cheong, and G. Blumberg, Covalency-driven collapse of strong spin-orbit coupling in face-sharing iridium octahedra, Phys. Rev. B **98**, 201105(R) (2018).

[34] Y. Wang, R. Wang, J. Kim, M. H. Upton, D. Casa, T. Gog, G. Cao, G. Kotliar, M. P. M. Dean, and X. Liu, Direct Detection of Dimer Orbitals in $Ba_5AlIr_2O_{11}$, Phys. Rev. Lett. **122**, 106401 (2019).

[35] Y. Klein, G. Rousse, F. Damay, F. Porcher, G. André, and I. Terasaki, Antiferromagnetic order and consequences on the transport properties of $Ba_4Ru_3O_{10}$, Phys. Rev. B **84**, 054439 (2011).

[36] S. V. Streltsov and D. I. Khomskii, Unconventional magnetism as a consequence of the charge disproportionation and the molecular orbital formation in $Ba_4Ru_3O_{10}$, Phys. Rev. B **86**, 064429 (2012).

[37] T. Igarashi, Y. Nogami, Y. Klein, G. Rousse, R. Okazaki, H. Taniguchi, Y. Yasui, and I. Terasaki, X-ray crystal structure analysis and Ru valence of $Ba_4Ru_3O_{10}$ single crystals, J. Phys. Soc. Jpn. **82**, 104603 (2013).

[38] G. Radtke, A. Saúl, Y. Klein, and G. Rousse, Magnetism of $Ba_4Ru_3O_{10}$ revealed by density functional calculations: Structural trimers behaving as coupled magnetic dimers, Phys. Rev. B **87**, 054436 (2013).

[39] T. Igarashi, R. Okazaki, H. Taniguchi, Y. Yasui, and I. Terasaki, Effects of the Ir impurity on the thermodynamic and transport properties of $Ba_4Ru_3O_{10}$, J. Phys. Soc. Jpn. **84**, 094601 (2015).

[40] J. Sannigrahi, A. Paul, A. Banerjee, D. Khalyavin, A. D. Hillier, K. Yokoyama, A. K. Bera, M. R. Lees, I. Dasgupta, S. Majumdar, and D. T. Adroja, Orbital effects and Affleck-Haldane-type spin dimerization in $Ba_4Ru_3O_{10}$, Phys. Rev. B **103**, 144431 (2021).

[41] S. Yamashita, Y. Nakazawa, M. Oguni, Y. Oshima, H. Nojiri, Y. Shimizu, K. Miyagawa, and K. Kanoda, Thermodynamic properties of a spin-1/2 spin-liquid state in a κ-type organic salt, Nat. Phys. **4**, 459 (2008).

[42] S. Yamashita, T. Yamamoto, Y. Nakazawa, M. Tamura, and R. Kato, Gapless spin liquid of an organic triangular compound evidenced by thermodynamic measurements, Nat. Commun. **2**, 275 (2011).

[43] See Supplemental Material at http://link.aps.org/supplemental/10.1103/PhysRevLett.129.207201 for bond valence sum analysis, additional details of the x-ray measurements and fittings, which also includes Refs. [44–49].

[44] X. Liu, M. P. M. Dean, J. Liu, S. G. Chiuzbăian, N. Jaouen, A. Nicolaou, W. G. Yin, C. R. Serrao, R. Ramesh, and H. Ding, Probing single magnon excitations in Sr_2IrO_4 using O K-edge resonant inelastic x-ray scattering, J. Phys. Condens. Matter **27**, 202202 (2015).

[45] D. I. Brown, *The Chemical Bond in Inorganic Chemistry: The Bond Valence Model* (Oxford University Press, New York, 2006).

[46] Bond valence parameters, https://www.iucr.org/resources/data/data-sets/bond-valence-parameters (accessed 2021-11-15).

[47] Y. Shen, G. Fabbris, H. Miao, Y. Cao, D. Meyers, D. G. Mazzone, T. A. Assefa, X. M. Chen, K. Kisslinger, D. Prabhakaran, A. T. Boothroyd, J. M. Tranquada, W. Hu, A. M. Barbour, S. B. Wilkins, C. Mazzoli, I. K. Robinson, and M. P. M. Dean, Charge Condensation and Lattice Coupling Drives Stripe Formation in Nickelates, Phys. Rev. Lett. **126**, 177601 (2021).

[48] O. K. Andersen, W. Klose, and H. Nohl, Electronic structure of Chevrel-phase high-critical-field superconductors, Phys. Rev. B **17**, 1209 (1978).

[49] I. Pérez Castillo, The exact two-spinon longitudinal dynamical structure factor of the anisotropic *XXZ* model, arXiv:2005.10729.

[50] J. Kim, D. Casa, M. H. Upton, T. Gog, Y.-J. Kim, J. F. Mitchell, M. van Veenendaal, M. Daghofer, J. van den Brink, G. Khaliullin, and B. J. Kim, Magnetic Excitation Spectra of Sr_2IrO_4 Probed by Resonant Inelastic X-Ray Scattering: Establishing Links to Cuprate Superconductors, Phys. Rev. Lett. **108**, 177003 (2012).

[51] X. Liu, V. M. Katukuri, L. Hozoi, W.-G. Yin, M. P. M. Dean, M. H. Upton, J. Kim, D. Casa, A. Said, T. Gog, T. F. Qi, G. Cao, A. M. Tsvelik, J. van den Brink, and J. P. Hill, Testing the Validity of the Strong Spin-Orbit-Coupling Limit for Octahedrally Coordinated Iridate Compounds in a Model System Sr_3CuIrO_6, Phys. Rev. Lett. **109**, 157401 (2012).

[52] J.-S. Caux, J. Mossel, and I. P. Castillo, The two-spinon transverse structure factor of the gapped Heisenberg antiferromagnetic chain, J. Stat. Mech. (2008) P08006.

[53] K. I. Kugel, D. I. Khomskii, A. O. Sboychakov, and S. V. Streltsov, Spin-orbital interaction for face-sharing octahedra: Realization of a highly symmetric SU(4) model, Phys. Rev. B **91**, 155125 (2015).

[54] D. C. Johnston, R. K. Kremer, M. Troyer, X. Wang, A. Klümper, S. L. Bud'ko, A. F. Panchula, and P. C. Canfield, Thermodynamics of spin $s = 1/2$ antiferromagnetic uniform and alternating-exchange Heisenberg chains, Phys. Rev. B **61**, 9558 (2000).

[55] Y. Savina, O. Bludov, V. Pashchenko, S. L. Gnatchenko, P. Lemmens, and H. Berger, Magnetic properties of the antiferromagnetic spin-$\frac{1}{2}$ chain system β-$TeVO_4$, Phys. Rev. B **84**, 104447 (2011).

[56] R. Coldea, D. A. Tennant, E. M. Wheeler, E. Wawrzynska, D. Prabhakaran, M. Telling, K. Habicht, P. Smeibidl, and K. Kiefer, Quantum criticality in an Ising chain: Experimental evidence for emergent E_8 symmetry, Science **327**, 177 (2010).

[57] M. Mena, N. Hänni, S. Ward, E. Hirtenlechner, R. Bewley, C. Hubig, U. Schollwöck, B. Normand, K. W. Krämer, D. F. McMorrow, and C. Rüegg, Thermal Control of Spin Excitations in the Coupled Ising-Chain Material $RbCoCl_3$, Phys. Rev. Lett. **124**, 257201 (2020).

[58] W. Yin, Frustration-driven unconventional phase transitions at finite temperature in a one-dimensional ladder Ising model, arXiv:2006.08921.

[59] A. Weichselbaum, W. Yin, and A. M. Tsvelik, Dimerization and spin decoupling in a two-leg Heisenberg ladder with frustrated trimer rungs, Phys. Rev. B **103**, 125120 (2021).

[60] EDRIXS website, https://github.com/NSLS-II/edrixs (accessed 2021-09-27).

[61] Y. L. Wang, G. Fabbris, M. P. M. Dean, and G. Kotliar, EDRIXS: An open source toolkit for simulating spectra of resonant inelastic x-ray scattering, Comput. Phys. Commun. **243**, 151 (2019).

[62] J. A. Mydosh, *Spin Glasses: An Experimental Introduction* (CRC Press, Boca Raton, 1993).

[63] R. Okuma, M. Kofu, S. Asai, M. Avdeev, A. Koda, H. Okabe, M. Hiraishi, S. Takeshita, K. M. Kojima, R. Kadono, T. Masuda, K. Nakajima, and Z. Hiroi, Dimensional reduction by geometrical frustration in a cubic antiferromagnet composed of tetrahedral clusters, Nat. Commun. **12**, 4382 (2021).

[64] Y. Shen *et al.*, Data Repository for: Emergence of Spinons in Layered Trimer Iridate $Ba_4Ir_3O_{10}$, 10.5281/zenodo.7249987 (2022).